ELECTROSPUN PLA/PCL/MPS NANOFIBROUS HYBRID COMPOSITE STRUCTURES FOR SUSTAINED DRUG RELEASE

Hazim J. Haroosh[1] and Yu Dong[2*]

[1] *Department of Chemical Engineering, Curtin University, Perth, WA 6845, Australia*
[2] *Department of Mechanical Engineering, Curtin University, Perth, WA 6845, Australia*
**Corresponding author's e-mail address: Y.Dong@curtin.edu.au*

Keywords: Electrospinning; Magnetic nanoparticles; Hybrid composites; Drug release

Abstract

Electrospun nanofibrous hybrid composite structures were prepared by blending poly(ε-caprolactone) (PCL) and poly(lactic acid) (PLA) solutions and then mixed with three different amounts (0.01, 0.1 and 1% wt/v) of iron oxide (Fe_3O_4) magnetic nanoparticles (MPs),carrying a therapeutic compound tetracycline hydrochloride (TCH) with the potential use for medical applications. The material system was investigated to understand how constituents of hybrid composites influenced the surface morphology to control drug release. It has been found that fibre properties are strongly related to the viscosity and electrical conductivity of prepared solutions. The addition of MPs increased moderately the solution viscosities and produced quite uniform nanofibres. The fibre diameter decreased with increasing MP concentration due to significantly enhanced solution conductivity in presence of MPs. Crystallinity and T_g of PCL and T_c of PLA decreased when MPs were mixed with the polymer blend. TCH loading appears to result in decreasing nanofibre diameters and cause to decrease T_g and T_m values of PCL. TCH release was accelerated by adding MPs to the blended polymers.

1 Introduction

Nanotechnology is dealing with synthetic and natural formations on the nanoscaled level, specifically in range of 1μm to 1 nm [1]. Diverse approaches have been undertaken in the recent years to produce nanostructures or nanomaterials, such as phase separation, self-assembly and electrospinning. Among these methods, electrospinning is a flexible polymer processing method to synthesise nanofibres in which a flow of a polymer melt or solution leads to a few jets to form the "Taylor cone" in the high electric voltage field [2]. These jets are driven out from the droplet surface and drawn into fibrous structures in the direction of the collecting plate. Electrospinning is a quite promising technique for many biomedical applications, especially in controlled drug delivery systems in the recent decades [3]. Besides, this kind of system has some significant benefits like nontoxic degradation in the body and sustained release of encapsulated drugs [4].

PLA is a semi-crystalline polymer and broadly used in a range of biomedical applications due to its dissolvability in common solvents, biodegradability, good mechanical properties and

biocompatibility [5]. PCL is also a semi-crystalline polymer largely used in tissue scaffolding due to its good drug permeability and slow biodegradability [6]. PCL is frequently applied as long term implantable incubators. Magnetic nanoparticles (Fe_3O_4) are inorganic materials, having low toxicity, super-paramagnetic ability, good biocompatibility, easy preparation [7] and better stability in atmosphere than metal nanoparticles [8].

Blending of PCL with PLA and MPs to produce electrospun hybrid nanocomposites may create a new drug delivery system which enables to directly deliver drugs to the targeted area of the body by external magnetic field. This paper aims to investigate effects of MPs on morphology, structure, crystallinity, thermal properties and drug release of hybrid nanocomposites by blending PCL solution with an equal volume ratio (1:1) of a PLA solution. The polymer solutions are well mixed with MPs at three amounts of 0.01, 0.1 and 1% wt/v, respectively.

2 Materials and methods

2.1 Materials

PLA 3051D (*MW* = 93,500 g/mol and T_g = 65.50°C) was supplied by NatureWorks, USA. PCL of *MW* = 80,000 g/mol, iron sulfate, iron nitrate, tetracycline hydrochloride (TCH, $C_{22}H_{24}N_2O_8 \cdot HCl$, *MW*=480.9 g/mol), phosphate buffer solution (PBS), chloroform and methanol were purchased from Sigma-Aldrich Ltd and used without any purification. Iron sulfate and iron nitrate were used to synthesise MPs whilst TCH and PBS acted as a model drug and a medium of drug release, respectively. Chloroform and methanol were employed as solvents for blended PLA and PCL.

2.2 Electrospinning

Electrospinning was carried out using 8% wt/v solution of PLA mixed with 15% wt/v solution of PCL. The PLA and PCL solutions were both mixed at a 1:1 volume ratio. The solvent used in all cases was a mixture of chloroform and methanol blended in a 2:1 volume ratio. The MPs were synthesised from iron sulfate ($FeSO_4$) and iron nitrate ($Fe(NO_3)_3$) and were added at 0.01, 0.1 and 1wt%/v to the blended polymer solution, which were mixed by using ultrasonication for 2 h. 5wt% of TCH was then mixed with 0.1wt%/v MP for 2h in methanol by using the similar ultrasonication and then added to the polymer solution. For electrospinning, the solution was transferred to 10 ml syringe mounted onto a syringe pump (A Fusion 100 syringe pump, Chemyx Inc. Stafford, TX USA) with a 20G metallic needle (0.584 mm inner diameter). The flow rate of the polymer solution was set at 2 ml/h, and the applied positive voltage was in range of 25–28 kV. The electrospinning process was conducted at 24ºC. The resulting fibres were collected on a ground collector covered by a flat aluminium foil. The distance between the needle tip and the target was 13 cm. The thickness of the fibre mats was measured between 330 and 450 μm.

2.3 In vitro drug release study

The drug-loaded fibre mat sample (2×2 cm^2) was incubated in a rotary shaker at 37 °C in 20 ml PBS (pH=7.4). After the required incubation time for drug release, the sample was transferred to 20 ml fresh buffer solution and the released TCH amount in the buffer solution was determined.

2.4 Characterisation techniques

Solution viscosity was evaluated with a Visco 88 portable viscometer from Malvern Instruments (UK). The electrical conductivity of the solution was measured by using a WP-81 Water Proof

Conductivity Meter (TPS, Australia). The nanofibre morphology was studied via an EVO 40XVP scanning electron microscope (SEM) (Germany) at an accelerating voltage of 5 kV. Before SEM observation, the samples were sputter-coated with platinum. Fibre diameter was calculated from the SEM images by using an image analysis tool in Zeiss smart SEM software. For each sample, measurements were made of a minimum of 150 fibres from multiple scanned SEM images and at a sampling rate of 15 fibres per image. XRD measurements of prepared samples were performed in a Bruker Discover 8 X-ray diffractometer (Germany) operated at 40kV and 40mA using the Cu-Kα radiation in a 2θ range from 5° to 40° at 0.05°/s. The *d*-spacing (*d*) corresponding to the XRD peak was determined from Bragg's equation, $n\lambda=2d\sin\theta$, where θ is the diffraction position, λ is the wavelength, which is 1.54 Å for a Cu target and n is an integer).Thermal analysis was performed using a DSC6000 Perkin Elmer (USA) with Cryofill liquid nitrogen cooling system. Approximately 10 mg of fibre mat was analysed during heating and cooling between 30°C and 200°C with a ramp rate of 10°C/min. The amount of TCH present in the release buffer was determined by a UV–vis spectrophotometer (JascoV-67) at the wavelength of 360 nm.

3 Results and discussion

The effects of MPs and TCH drug on the morphology of electrospun hybrid composites are demonstrated in Figure 1, along with the fibre diameters measured by the imaging analysis in Table 1. With increasing the MPs concentration from 0.01 wt%/v to 0.1 wt%/v, the produced fibres in this nanocompsite system become quite uniform, as seen from Figures 1(b) and (c), and the fibre diameter moderately decreases from 711 nm to 685 nm as opposed to 814 nm without MPs. This decreasing tendency continues at MPs of 1 wt%/v with the average diameter of 583 nm. But the non-uniform fibre morphology evidently takes place and the typical bead defects on the fibres are detected, Figure 1(d). These beads might be seen as the aggregates of MPs that normally do not exist in hybrid nanocomposites with low MPs concentrations. On the other hand, the addition of 5 wt% TCH into nanocomposites with 0 wt%/v and 0.1 wt%/v MPs, to a further extent, facilitates the reduction of fibre diameter, as compared to their corresponding counterparts without TCH. In view of two primary parameters of solution viscosity and electrical conductivity in the electrospinning process, both parameters are enhanced remarkably when the MPs concentration increases from 0 wt%/v to 1 wt%/v, Figure 2. As expected, the additional cationic drug TCH further increases the solution conductivity as compared to those without TCH, Figure 2(b). This infers that electrical conductivity plays a relatively dominant role in determining fiber morphology though the addition of MPs increases the viscosity of the solution.

MPs	**MP 0%**	**MP 0.01%**	**MP 0.1%**	**MP 1%**	**MP 0% and TCH**	**MP 0.1% and TCH**
PLA: PCL	814 (±15)	711 (±15)	685 (±20)	583 (±25)	623 (±15)	562 (±20)

Note: *All fibre diameters are in nm and standard deviations are numbers in the brackets.*

Table 1.Summary of the average fibre diameters for hybrid composites with MPs and TCH

It was reported that decreasing the viscosity of the spinning solution resulted in a decrease in the fibre diameter whilst higher electrical conductivity produced fibres with smaller diameters [9]. The decreased nanofibre diameters found in this study could be ascribed to the predominant

effect of significant increase of electrical conductivity on the fibre morphological structure relative to a modest increase of solution viscosity. In terms of the effect of electrical conductivity, as shown in Figure 2(b), an increase in the amount of MPs led to increase in the conductivity apparently due to the addition of ionic irons in MPs. More importantly, the use of drug TCH can further enhance the electrical conductivity of electrospun hybrid composites significantly especially at the MP concentrations of 0-0.1 wt%/v with wider bands of difference. As a matter of fact, the increased electrical conductivity inevitably produces more electric charges that are carried by the electrospining jet. Consequently, higher repulsive forces are imposed to the jet in order to elongate the jet materials into fibrous structures under the electrical field [10]. Besides, by increasing the electrical conductivity, the draw rate and large draw ratio of the jet in its bending instability area can increase during electrospinning. Hence, the jet path becomes longer and more stretching of the solution is induced. Both higher repulsive forces and greater bending instability could contribute to electrospun fibres with smaller diameters [11, 12].

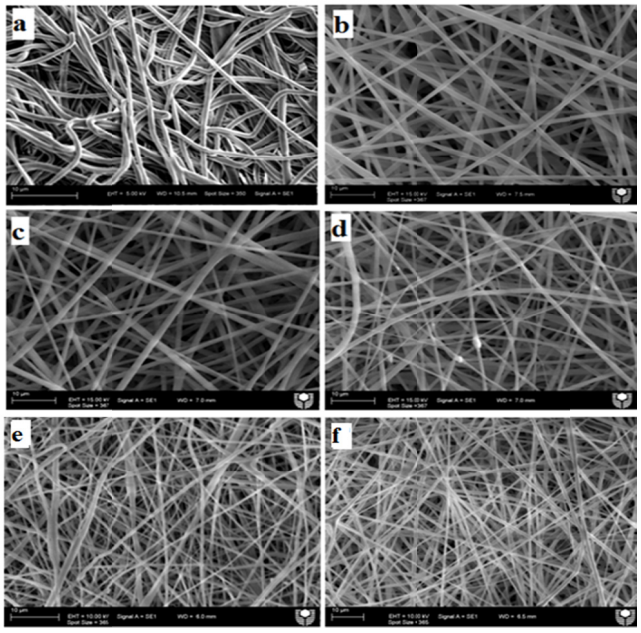

Figure. 1. SEM images of electrospun PLA: PCL (1:1) fibres blended with pure MPs: (a) 0% MPs, (b) 0. 01% MPs, (c) 0.1% MPs, (d) 1% MPs, (e) 0% MPs with TCH and (f) 0.1% MPs with TCH.

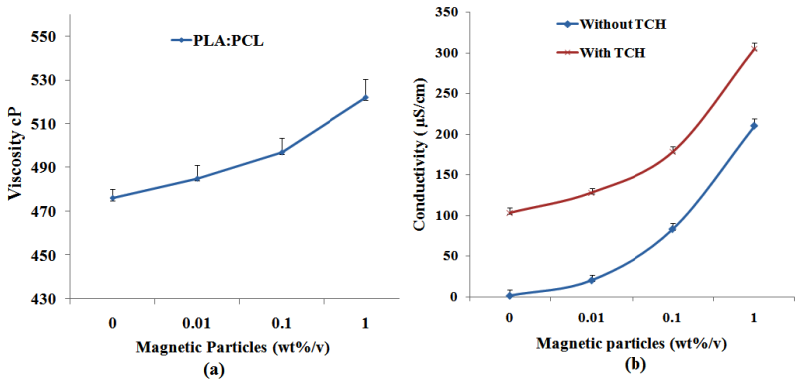

Figure 2. Effect of MPs concentration on (a) viscosity of PLA: PCL blended polymer solution and (b) electrical conductivity of PLA: PCL blended polymer solution with/without TCH.

3.1 Crystallinity and thermal properties

Figures 3(a) and (b) demonstrate the XRD patterns obtained for hybrid composites and MPs to identify their crystalline structures, respectively. The peaks labelled with the XRD reflection and the crystal planes (*hkl*), corresponding to the main crystalline peaks, were obtained from the DICVOL program in the FullProf Suite software package [13]. The diffraction pattern of pure MPs, as shown in Figure 3(b), presents six characteristic XRD peaks detected at 2θ = 30.1°, 34.3°, 43.1°, 53.4°, 57.2°,and 63.2°, which are corresponding to the (220), (311), (400), (422), (511) and (440) basal reflections with *d*-spacing values of 0. 29, 0.25, 0.21, 0.17, 0.16 and 0.14 nm, respectively. These calculated *d*-spacing values are in good accordance with those of typical magnetite (Fe_3O_4).The average crystal size (L) of MPs, calculated from the half-width of the diffraction peaks using the Scherrer relation [14], is on the order of 20±5 nm.

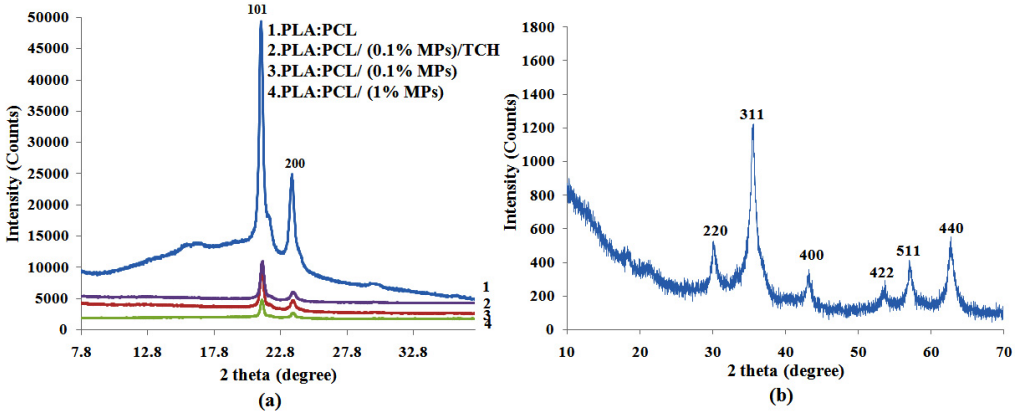

Figure 3. XRD patterns for (a) electrospun hybrid composites and (b) MPs

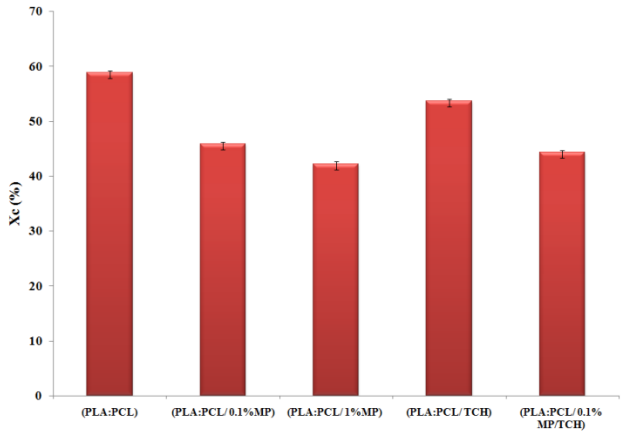

Figure 4. Degree of crystallinity (X_c) for PLA: PCL hybrid composites (calculated from XRD data).

The XRD patterns of PLA:PCL hybrid composites are also illustrated in Figure 3(a). Their peaks appear at 2θ = 21.39° and 23.58°, which are corresponding to (101) and (200) basal reflections with *d*-spacing values of 0.42 and 0.38 nm, respectively. The additions of MPs and TCH have very minor effect on the alteration of intensity peak positions. It can be noted from Figure 4 that without TCH, the crystallinity of PLA: PCL based hybrid composites decrease significantly by increasing the MPs concentration. Such decreasing tendency might be explained by the

abundance of nucleation cores that produce a proliferation of tiny crystallites to offer a low degree of overall crystallinity [15]. Additionally, the presence of 5% TCH in hybrid composites also leads to a moderate decrease of degree of crystallinity as compared to PLA: PCL counterpart. The crystallinity is reduced further when 0.1% MPs is concurrently used in hybrid PLA: PCL composites with 5% TCH, which is even lower than that of PLA: PCL composites with 0.1% MPs. Both MPs and TCH appear to greatly accelerate the nucleation speed. Hence, this phenomenon causes a shorter period than the required time for the disentanglement of molecular chains because the resulting degree of crystallinity is influenced by the restricted mobility of polymer chains, which prevents a good growth of the developed crystals.

Sample	T_g(°C) **PCL**	T_m(°C) **PCL**	T_C (°C) **PLA**	T_m(°C) **PLA**
PLA : PCL	–52.19	63.75	83.97	152.54
PLA : PCL (1% MPs)	–58.17	62.2	81.63	151.44
PLA : PCL (0.1% MPs)	–53.01	61.47	82.64	151.72
PLA : PCL / TCH	–58.48	59.64	105.77	151.93
PLA : PCL/ (0.1% MPs)/TCH	–60.47	59.16	101.79	149.41

DSC tests were repeated for three sets of samples. The standard deviations for the T_g and T_m values are less than 0.5%.

Table 2. DSC results for PLA: PCL hybrid composites with MPs and TCH

The DSC results shown in Table 2 indicate that the glass transition temperature (T_g) of PCL decreases remarkably and there was a slight decline in melting temperature (T_m) values of both PLA and PCL by increasing the MPs concentrations from 0 wt%/v to 1wt%/v as well as adding 5% TCH. The decrease of T_g is ascribed to the dual effect of incorporation of magnetite particles with the anisotropic character, in good accordance with the previous work [16], and blending of the drug TCH with the low molecular weight. The TCH molecules have short chains, which results in the decreased packing density of polymer chains and thus facilitates the chain mobility leading to the lower T_g. Moreover, electrospinning process and resulting fibre diameters can also influence the mobility direction of polymer chains, causing the difference in T_g [17]. The embedded MPs in PCL: PLA have been found to slightly decrease the crystallisation temperature (T_c) of PLA. The nucleating role of MPs to promote the heterogeneous nucleation of polymer molecules are not strongly revealed, which might be attributed to the low concentration of MPs. The T_g of PLA within the blend is difficult to be observed because it easily overlaps with the melting peak of PCL. Conversely, the use of TCH within hybrid composites shows a significant increase of T_c at over 102ºC as opposed to 84ºC of PLA in PLA: PCL samples. This phenomenon implies that low molecular weight TCH can hinder the cold crystallisation process of PLA, acting as an anti-nucleating agent which, however, possesses the opposite role of MPs.

3.2 In vitro drug release study

TCH release profiles from electrospun hybrid composites with and without MPs are demonstrated in Figure 5. Both composite mats proved to have a sustained drug release performance though a certain degree of fast drug release was found within the first 5 h (46% for PLA:PCL/MPs samples vs. 42% for PLA:PCL samples). This is followed by a gradually steady

release in the total evaluation over 10 days' release test. The fast release is associated with the electrospinning process which includes the fast evaporation of the solvent and the high ionic interactions leading to the drug location on the surfaces of electrospun fibres. It was found that TCH was released more rapidly when adding MPs to the blended polymer and the difference of cumulative release (%) becomes more prevalent compared to those composites without MPs especially after 50 h. This finding is quite convincing that TCH release was due to two main factors of the drug diffusion through the pores and biodegradation of electrospun fibres. The incorporation of MPs due to their nanoscaled sizes, leads to the increased fibre porosity [18] which is then capable of accelerating the TCH release. In addition, the small diameters of PLA: PCL/MPs hybrid composite fibrous structures compare with PLA:PCL counterparts certainly promote the surface area, which offers the short diffusion distance with a fast TCH release. Moreover, the low crystallinity of PLA: PCL/MPs hybrid composites can enhance the fibre degradability on the long term of TCH release.

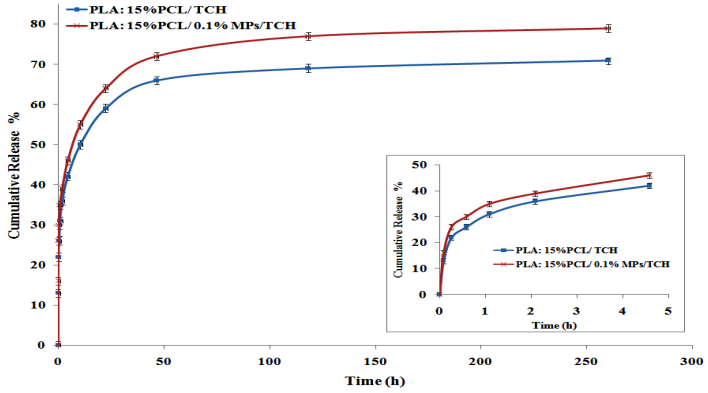

Figure 5.TCH release profiles from PLA:PCL and PLA: PCL/MPs hybrid composites.

4 Conclusions

Increasing the MPs concentrations produced hybrid nanocomposites with decreased average fibre diameters. Whereas, adding drug (TCH) to the nanocomposite resulted in the smaller fibres. This effect was attributed to the higher solution viscosity and electrical conductivity from which the latter is more dominant. Crystallinity and T_g of PCL decreased when MPs were mixed with the blended polymers. In addition, MPs led to a reasonable decrease in the values of T_c of PLA in blending. The use of TCH caused to decrease T_g and T_m values of PCL and also offered a slightly change in T_m values of PLA. The addition of MPs to the blended polymers was found to accelerate TCH release compared to the PLA: PCL polymer blend.

5 Acknowledgements

The PhD scholarship awarded by Iraqi government to Mr. Hazim J. Haroosh and Curtin Internal Research Grants (IRG) 2010 (Project No.: 47604) to Dr. Yu Dong are gratefully acknowledged. Special thanks are also indebted to Dr. Deeptangshu Chaudhary for initial constructive technical supports and discussions on magnetic particles.

References

[1] Qi R., Guo R., Shen M., Cao X., Zhang L., Xu J., et al. Electrospun poly (lactic-co-glycolic acid)/halloysite nanotube composite nanofibers for drug encapsulation and sustained release. *J. Mater. Chem.*, **20**, pp. 10622-10629 (2010).

[2] Ji Y., Ghosh K., Li B., Sokolov J., Clark R., Rafailovich M. Dual Syringe Reactive Electrospinning of Cross Linked Hyaluronic Acid Hydrogel Nanofibers for Tissue Engineering Applications. *Macromo. Biosci.*,**6**, pp.811-817 (2006).
[3] Kenawy E., Abdel-Hay F., El-Newehy M., Wnek G. Processing of polymer nanofibers through electrospinning as drug delivery systems. *Mater. Chem. Phys.*, **113**, pp. 296-302 (2009).
[4] Yang D., Li Y., Nie J. Preparation of gelatin/PVA nanofibers and their potential application in controlled release of drugs. *Carbohydr. Polym.*,**7**, pp. 538-543 (2007).
[5] Cui W., Li X., Zhu X., Yu G., Zhou S., Weng J. Investigation of drug release and matrix degradation of electrospun poly (DL-lactide) fibers with paracetanol inoculation. *Biomacromolecules*, **7**, pp. 1623-1629 (2006).
[6] Han J., Branford-White C., Zhu L.. Preparation of poly (ε-caprolactone)/poly (trimethylene carbonate) blend nanofibers by electrospinning. *Carbohydr. Polym.*, **79**, pp. 214-218 (2010).
[7] Lv G., He F., Wang X., Gao F., Zhang G., Wang T., et al. Novel nanocomposite of nano Fe3O4 and polylactide nanofibers for application in drug uptake and induction of cell death of leukemia cancer cells. *Langmuir*, **24**, pp. 2151-2156 (2008).
[8] Zhang D., Karki A.B., Rutman D., Young D.P., Wang A., Cocke D., et al. Electrospun polyacrylonitrile nanocomposite fibers reinforced with Fe_3O_4 nanoparticles: Fabrication and property analysis. *Polymer*, **50**, pp. 4189-4198 (2009).
[9] Haroosh H.J., Chaudhary D.S., Dong Y. Electrospun PLA/PCL fibers with tubular nanoclay: Morphological and structural analysis. *J. Appli. Polym. Sci.*, **124**, pp. 3930-3939 (2012).
[10] Zamani M., Morshed M., Varshosaz J., Jannesari M. Controlled release of metronidazole benzoate from poly (ε-caprolactone) electrospun nanofibers for periodontal diseases. *Eur. J. Pharm. Biopharm.*, **75**, pp. 179-185 (2010).
[11] Lee G., Song J., Yoon K.. Controlled wall thickness and porosity of polymeric hollow nanofibers by coaxial electrospinning. *Macromol. Res.*, **18**, pp. 571-576 (2010).
[12] Saraf A., Lozier G., Haesslein A., Kasper F., Raphael R., Baggett L., et al. Fabrication of Nonwoven Coaxial Fiber Meshes by Electrospinning. *Tissue Eng. Part C: Methods*, **15**, pp. 333-344 (2009).
[13] Boultif A., Louer D. Powder pattern indexing with the dichotomy method. *J. Appl. Crystallogr.*, **37**, pp. 724-731(2004).
[14] Ning N., Yin Q., Luo F., Zhang Q., Du R., Fu Q. Crystallization behavior and mechanical properties of polypropylene/halloysite composites. *Polymer*, **48**, pp. 7373-7384 (2007).
[15] Lee J.H., Park T.G., Park H.S., Lee D.S., Lee Y.K., Yoon S.C., et al. Thermal and mechanical characteristics of poly (L-lactic acid) nanocomposite scaffold. *Biomaterials,* **24**, pp. 2773-2778 (2003).
[16] Kumar R.V., Koltypin Y., Cohen Y.S., Cohen Y., Aurbach D., Palchik O., et al. Preparation of amorphous magnetite nanoparticles embedded in polyvinyl alcohol using ultrasound radiation. *J. Mater. Chem.*, **10**, pp.1125-1129 (2000).
[17] Picciani P., Medeiros E., Pan Z., Wood D., Orts W., Mattoso L., et al. Structural, Electrical, Mechanical, and Thermal Properties of Electrospun Poly (lactic acid)/Polyaniline Blend Fibers. *Macromol. Mater. Eng.,***295**, pp. 618-627 (2010).
[18] Mikołajczyk T., Olejnik M. Effects of spinning conditions on structure and properties of multifunctional fibers of polyimidoamide nanocomposites. *J. Appli. Polym. Sci.*, **100**, pp. 3323-3331(2006).